

Principal Bit Analysis: Autoencoding with Schur-Concave Loss

Sourbh Bhadane*
Cornell University
snb62@cornell.edu

Aaron B. Wagner*
Cornell University
wagner@cornell.edu

Jayadev Acharya*
Cornell University
acharya@cornell.edu

November 19, 2021

Abstract

We consider a linear autoencoder in which the latent variables are quantized, or corrupted by noise, and the constraint is Schur-concave in the set of latent variances. Although finding the optimal encoder/decoder pair for this setup is a nonconvex optimization problem, we show that decomposing the source into its principal components is optimal. If the constraint is strictly Schur-concave and the empirical covariance matrix has only simple eigenvalues, then any optimal encoder/decoder must decompose the source in this way. As one application, we consider a strictly Schur-concave constraint that estimates the number of bits needed to represent the latent variables under fixed-rate encoding, a setup that we call *Principal Bit Analysis (PBA)*. This yields a practical, general-purpose, fixed-rate compressor that outperforms existing algorithms. As a second application, we show that a prototypical autoencoder-based variable-rate compressor is guaranteed to decompose the source into its principal components.

1 Introduction

Autoencoders are an effective method for representation learning and dimensionality reduction. Given a centered dataset $x_1, x_2, \dots, x_n \in \mathbb{R}^d$ (i.e., $\sum_i x_i = 0$), an autoencoder (with *latent dimension* $k \leq d$) consists of an *encoder* $f : \mathbb{R}^d \mapsto \mathbb{R}^k$ and a *decoder* $g : \mathbb{R}^k \mapsto \mathbb{R}^d$. The goal is to select f and g from prespecified classes \mathcal{C}_f and \mathcal{C}_g respectively such that if a random point x is picked from the data set then $g(f(x))$ is close to x in some sense, for example in mean squared error. If \mathcal{C}_f and \mathcal{C}_g consist of linear mappings then the autoencoder is called a *linear autoencoder*.

Autoencoders have achieved striking successes when f and g are selected through training from the class of functions realized by multilayer perceptrons of a given architecture [HS06]. Yet, the canonical autoencoder formulation described above has a notable failing, namely that for linear autoencoders, optimal choices of f and g do not necessarily identify the principal components of the dataset; they merely identify the principal subspace [BK88, BH89]. That is, the

*This research was supported by the US National Science Foundation under grants CCF-2008266, CCF-1934985, CCF-1617673, CCF-1846300, CCF-1815893 and the US Army Research Office under grant W911NF-18-1-0426.

components of $f(x)$ are not necessarily proportional to projections of x against the eigenvectors of the covariance matrix

$$K \stackrel{\text{def}}{=} \frac{1}{n} \sum_{i=1}^n x_i \cdot x_i^\top, \quad (1)$$

which we assume without loss of generality is full rank. Thus, linear autoencoders do not recover Principal Component Analysis (PCA). The reason for this is that both the objective (the distortion) and the constraint (the dimensionality of the latents) are invariant to an invertible transformation applied after the encoder with its inverse applied before the decoder. It is desirable for linear autoencoders to recover PCA for two reasons. First, from a representation learning standpoint, it guarantees that the autoencoder recovers uncorrelated features. Second, since a conventional linear autoencoder has a large number of globally optimal solutions corresponding to different bases of the principal subspace, it is preferable to eliminate this indeterminism.

Autoencoders are sometimes described as “compressing” the data [San12, BK88, LZW⁺21, Bis06], even though f can be invertible even when $k < d$. We show that by embracing this compression-view, one can obtain autoencoders that are able to recover PCA. Specifically, we consider linear autoencoders with quantized (or, equivalently, noisy) latent variables with a constraint on the estimated number of bits required to transmit the quantized latents under fixed-rate coding. We call this problem *Principal Bit Analysis (PBA)*. The constraint turns out to be a strictly Schur-concave function of the set of variances of the latent variables (see the supplementary for a review of Schur-concavity). Although finding the optimal f and g for this loss function is a nonconvex optimization problem, we show that for any strictly Schur-concave loss function, an optimal f must send projections of the data along the principal components, assuming that the empirical covariance matrix of the data has only simple eigenvalues. That is, imposing a strictly Schur-concave loss in place of a simple dimensionality constraint suffices to ensure recovery of PCA. The idea is that the strict concavity of the loss function eliminates the rotational invariance described above. As we show, even a slight amount of “curvature” in the constraint forces the autoencoder to spread the variances of the latents out as much as possible, resulting in recovery of PCA. If the loss function is merely Schur-concave, then projecting along the principal components is optimal, but not necessarily uniquely so.

Using this theorem, we can efficiently solve PBA. We validate the solution experimentally by using it to construct a fixed-rate compression algorithm for arbitrary vector-valued data sources. We find that the PBA-derived compressor beats existing linear, fixed-rate compressors both in terms of mean squared error, for which it is optimized, and in terms of the structural similarity index measure (SSIM) and downstream classification accuracy, for which it is not.

A number of variable-rate multimedia compressors have recently been proposed that are either related to, or directly inspired by, autoencoders [TAL18, TVJ⁺17, BLS16, TOH⁺16, TSCH17, RB17, HRTC19, AMT⁺17, BMS⁺18, ZCG⁺18, ATM⁺19, BCM⁺20]. As a second application of our result, we show that for Gaussian sources, a linear form of such a compressor is guaranteed to recover PCA. Thus we show that ideas from compression can be fruitfully fed back into the original autoencoder problem.

The contributions of the paper are

- We propose a novel linear autoencoder formulation in which the constraint is Schur-concave. We show that this generalizes conventional linear autoencoding.
- If the constraint is strictly Schur-concave and the covariance matrix of the data has only

simple eigenvalues, then we show that the autoencoder provably recovers PCA, providing a new remedy for a known limitation of linear autoencoders.

- We use the new linear autoencoder formulation to efficiently solve a fixed-rate compression problem that we call *Principal Bit Analysis (PBA)*.
- We demonstrate experimentally that PBA outperforms existing fixed-rate compressors on a variety of data sets and metrics.
- We show that a linear, variable-rate compressor that is representative of many autoencoder-based compressors in the literature effectively has a strictly Schur-concave loss, and therefore it recovers PCA.

Related Work. Several recent works have examined how linear autoencoders can be modified to guarantee recovery of PCA. Most solutions involve eliminating the invariant global optimal solutions by introducing regularization of some kind. [OSWS20] propose a loss function which adds k penalties to recover the k principal directions, each corresponding to recovering up to the first $i \leq k$ principal directions. [KBGS19] show that ℓ_2 regularization helps reduce the symmetry group to the orthogonal group. [BLSG20] further break the symmetry by considering non-uniform ℓ_2 regularization and deterministic dropout. [LNP19] consider a nonlinear autoencoder with a covariance loss term to encourage finding orthogonal directions. Recovering PCA is an important problem even in the stochastic counterpart of autoencoders. [LTGN19] analyze linear variational autoencoders (VAEs) and show that the global optimum of its objective is identical to the global optimum of log marginal likelihood of probabilistic PCA (pPCA). [RZM19] analyze an approximation to the VAE loss function and show that the linear approximation to the decoder is orthogonal.

Our result on variable-rate compressors is connected to the sizable recent literature on compression using autoencoder-like architectures. Representative contributions to the literature were noted above. Those works focus mostly on the empirical performance of deep, nonlinear networks, with a particular emphasis on finding a differentiable proxy for quantization so as to train with stochastic gradient descent. In contrast, this work considers provable properties of the compressors when trained perfectly.

Notation. We denote matrices by bold capital letters e.g. M , and vectors by bold small, e.g. v . The j^{th} column of a matrix M is denoted by m_j and the j^{th} entry of a vector v by $[v]_j$. We denote the set $\{1, 2, \dots, d\}$ by $[d]$. A sequence a_1, a_2, \dots, a_n is denoted by $\{a_i\}_{i=1}^n$. We denote the zero column by $\mathbf{0}$. Logarithms without specified bases denote natural logarithms.

Organization. The balance of the paper is organized as follows. We describe our constrained linear autoencoder framework in Section 2. This results in an optimization problem that we solve for any Schur-concave constraint in Section 2.1. In Section 3, we recover linear autoencoders and PBA under our framework. We apply the PBA solution to a problem in variable-rate compression of Gaussian sources in Section 4. Section 5 contains experiments comparing the performance of the PBA-based fixed-rate compressor against existing fixed-rate linear compressors on image and audio datasets.

2 Linear Autoencoding with a Schur-Concave Constraint

Throughout this paper we consider \mathcal{C}_f and \mathcal{C}_g to be the class of linear functions. The functions $f \in \mathcal{C}_f$ and $g \in \mathcal{C}_g$ can then be represented by d -by- d matrices, respectively, which we denote by \mathbf{W} and \mathbf{T} , respectively. Thus we have

$$f(\mathbf{x}) = \mathbf{W}^\top \mathbf{x} \quad (2)$$

$$g(\mathbf{x}) = \mathbf{T} \mathbf{x}. \quad (3)$$

We wish to design \mathbf{W} and \mathbf{T} to minimize the mean squared error when the latent variables $\mathbf{W}^\top \mathbf{x}$ are quantized, subject to a constraint on the number of bits needed to represent the quantized latents. We accomplish this via two modifications of the canonical autoencoder. First, we perturb the d latent variables with zero-mean additive noise with covariance matrix $\sigma^2 \mathbf{I}$, which we denote by ε . Thus the input to the decoder is

$$\mathbf{W}^\top \mathbf{x} + \varepsilon \quad (4)$$

and our objective is to minimize the mean squared error

$$\frac{1}{n} \sum_{i=1}^n \mathbb{E}_{\varepsilon} \left[\left\| \mathbf{x}_i - \mathbf{T} \left(\mathbf{W}^\top \mathbf{x}_i + \varepsilon \right) \right\|_2^2 \right]. \quad (5)$$

This is equivalent to quantizing the latents, in the following sense [ZF92]. Let $Q(\cdot)$ be the function that maps any real number to its nearest integer and ε be a random variable uniformly distributed over $[-1/2, 1/2]$. Then for X independent of ε , the quantities $Q(X + \varepsilon) - \varepsilon$ and $X + \varepsilon$ have the same joint distribution with X . Thus (5) is exactly the mean squared error if the latents are quantized to the nearest integer and $\sigma^2 = \frac{1}{12}$, assuming that the quantization is dithered. The overall system is depicted in Fig. 1.

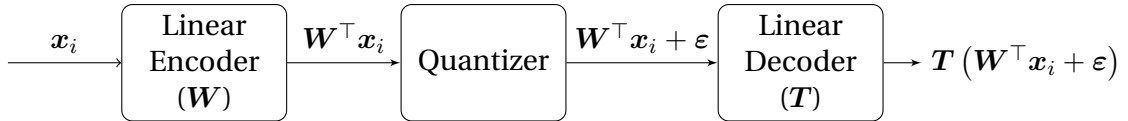


Figure 1: Compression Block Diagram

We wish to constrain the number of bits needed to describe the latent variables. We assume that the j th quantized latent is clipped to the interval

$$\left(-\frac{\sqrt{(2a)^2 \mathbf{w}_j^\top \mathbf{K} \mathbf{w}_j + 1}}{2}, \frac{\sqrt{(2a)^2 \mathbf{w}_j^\top \mathbf{K} \mathbf{w}_j + 1}}{2} \right],$$

where $a > 0$ is a hyperparameter and the covariance matrix \mathbf{K} is as defined in (1). The idea is that for sufficiently large a , the interval

$$\left(-a \sqrt{\mathbf{w}_j^\top \mathbf{K} \mathbf{w}_j}, a \sqrt{\mathbf{w}_j^\top \mathbf{K} \mathbf{w}_j} \right]$$

contains the latent with high probability, and adding 1 accounts for the expansion due to the dither. The number of bits needed for the j th latent is then

$$\log \left(\sqrt{4a^2 \mathbf{w}_j^\top \mathbf{K} \mathbf{w}_j} + 1 \right) = \frac{1}{2} \log \left(4a^2 \mathbf{w}_j^\top \mathbf{K} \mathbf{w}_j + 1 \right). \quad (6)$$

We arrive at our optimization problem:

$$\begin{aligned} \inf_{\mathbf{W}, \mathbf{T}} \quad & \frac{1}{n} \sum_{i=1}^n \mathbb{E}_{\varepsilon} \left[\left\| \mathbf{x}_i - \mathbf{T} \left(\mathbf{W}^\top \mathbf{x}_i + \varepsilon \right) \right\|_2^2 \right] \\ \text{subject to} \quad & R \geq \sum_{j=1}^d \frac{1}{2} \log \left(4a^2 \mathbf{w}_j^\top \mathbf{K} \mathbf{w}_j + 1 \right). \end{aligned} \quad (7)$$

Note that the function

$$\{\mathbf{w}_j^\top \mathbf{K} \mathbf{w}_j\}_{j=1}^d \mapsto \sum_{j=1}^d \frac{1}{2} \log \left(4a^2 \mathbf{w}_j^\top \mathbf{K} \mathbf{w}_j + 1 \right)$$

is strictly Schur-concave (see Appendix A for a brief review of Schur-concavity). Our first result only requires that the constraint is Schur-concave in the set of latent variances, so we will consider the more general problem

$$\begin{aligned} \inf_{\mathbf{W}, \mathbf{T}} \quad & \frac{1}{n} \sum_{i=1}^n \mathbb{E}_{\varepsilon} \left[\left\| \mathbf{x}_i - \mathbf{T} \left(\mathbf{W}^\top \mathbf{x}_i + \varepsilon \right) \right\|_2^2 \right] \\ \text{subject to} \quad & R \geq \rho \left(\left\{ \mathbf{w}_j^\top \mathbf{K} \mathbf{w}_j \right\}_{j=1}^d \right) \end{aligned} \quad (8)$$

where $\rho(\cdot)$ is any Schur-concave function.

Expressing the objective in (8) in terms of \mathbf{K} , the optimization problem reduces to

$$\begin{aligned} \inf_{\mathbf{W}, \mathbf{T}} \quad & \text{tr}(\mathbf{K}) - 2\text{tr}(\mathbf{K} \mathbf{W} \mathbf{T}^\top) + \text{tr}(\mathbf{T} (\mathbf{W}^\top \mathbf{K} \mathbf{W} + \sigma^2 \mathbf{I}) \mathbf{T}^\top) \\ \text{subject to} \quad & R \geq \rho \left(\left\{ \mathbf{w}_j^\top \mathbf{K} \mathbf{w}_j \right\}_{j=1}^d \right). \end{aligned} \quad (9)$$

Since \mathbf{T} does not appear in the rate constraint, the optimal \mathbf{T} can be viewed as the Linear Least Squares Estimate (LLSE) of a random \mathbf{x} given $\mathbf{W}^\top \mathbf{x} + \varepsilon$. Therefore, the optimal decoder, \mathbf{T}^* for a given encoder \mathbf{W} is (e.g. [Kay98]):

$$\mathbf{T}^* = \mathbf{K} \mathbf{W} (\mathbf{W}^\top \mathbf{K} \mathbf{W} + \sigma^2 \mathbf{I})^{-1}. \quad (10)$$

Substituting for \mathbf{T} in (9) yields an optimization problem over only \mathbf{W}

$$\begin{aligned} \inf_{\mathbf{W}} \quad & \text{tr}(\mathbf{K}) - \text{tr}(\mathbf{K} \mathbf{W} (\mathbf{W}^\top \mathbf{K} \mathbf{W} + \sigma^2 \mathbf{I})^{-1} \mathbf{W}^\top \mathbf{K}) \\ \text{subject to} \quad & R \geq \rho \left(\left\{ \mathbf{w}_j^\top \mathbf{K} \mathbf{w}_j \right\}_{j=1}^d \right). \end{aligned} \quad (11)$$

This problem is nonconvex in general. In the following subsection, we prove a structural result about the problem for a Schur-concave ρ . Namely, we show that the nonzero rows of \mathbf{W} must be eigenvectors of \mathbf{K} . In Section 3, we solve the problem for the specific choice of ρ in (7). We also show how this generalizes conventional linear autoencoders.

2.1 Optimal Autoencoding with a Schur-Concave Constraint

The following is the main theoretical result of the paper.

Theorem 1. *For Schur-concave $\rho : \mathbb{R}_{\geq 0}^d \rightarrow \mathbb{R}_{\geq 0}$ and $R > 0$, the set of matrices whose nonzero columns are eigenvectors of the covariance matrix \mathbf{K} is optimal for (11). If ρ is strictly Schur-concave and \mathbf{K} contains distinct eigenvalues, this set contains all optimal solutions of (11).*

Proof. Let the eigenvalues of \mathbf{K} be $\{\sigma_i^2\}_{i=1}^d$ with $\sigma_1^2 \geq \sigma_2^2 \geq \dots \geq \sigma_d^2$. Let the eigendecomposition of \mathbf{K} be given by $\mathbf{K} = \mathbf{U}\mathbf{\Sigma}\mathbf{U}^\top$ where \mathbf{U} is an orthogonal matrix whose columns are the eigenvectors of \mathbf{K} and $\mathbf{\Sigma}$ is a diagonal matrix with entries $\{\sigma_i^2\}_{i=1}^d$.

We first prove that the optimal value of (11) can be achieved by \mathbf{W} such that $\mathbf{W}^\top \mathbf{K} \mathbf{W}$ is a diagonal matrix. Let $\tilde{\mathbf{W}} = \mathbf{W} \mathbf{Q}$ where \mathbf{Q} is the orthogonal matrix obtained from the eigendecomposition of $\mathbf{W}^\top \mathbf{K} \mathbf{W}$ i.e.,

$$\mathbf{W}^\top \mathbf{K} \mathbf{W} = \mathbf{Q} \mathbf{\Lambda} \mathbf{Q}^\top,$$

where $\mathbf{\Lambda}$ is a diagonal matrix formed from the eigenvalues of $\mathbf{W}^\top \mathbf{K} \mathbf{W}$. Note that

$$\begin{aligned} \text{tr} \left(\mathbf{K} \tilde{\mathbf{W}} \left(\tilde{\mathbf{W}}^\top \mathbf{K} \tilde{\mathbf{W}} + \sigma^2 \mathbf{I} \right)^{-1} \tilde{\mathbf{W}}^\top \mathbf{K} \right) &= \text{tr} \left(\mathbf{K} \mathbf{W} \mathbf{Q} \left(\mathbf{\Lambda} + \sigma^2 \mathbf{I} \right)^{-1} \mathbf{Q}^\top \mathbf{W}^\top \mathbf{K} \right) \\ &= \text{tr} \left(\mathbf{K} \mathbf{W} \left(\mathbf{Q} \mathbf{\Lambda} \mathbf{Q}^\top + \sigma^2 \mathbf{Q} \mathbf{Q}^\top \right)^{-1} \mathbf{W}^\top \mathbf{K} \right). \end{aligned}$$

Since $\mathbf{Q} \mathbf{\Lambda} \mathbf{Q}^\top = \mathbf{W}^\top \mathbf{K} \mathbf{W}$ and $\mathbf{Q} \mathbf{Q}^\top = \mathbf{I}$, the objective remains the same. We now show that the constraint is only improved. Denoting the eigenvalues of $\mathbf{W}^\top \mathbf{K} \mathbf{W}$ by $\{\nu_j\}_{j=1}^d$, we have

$$\rho \left(\left\{ \tilde{\mathbf{w}}_j^\top \mathbf{K} \tilde{\mathbf{w}}_j \right\}_{j=1}^d \right) = \rho \left(\left\{ \mathbf{q}_j^\top \mathbf{W}^\top \mathbf{K} \mathbf{W} \mathbf{q}_j \right\}_{j=1}^d \right) = \rho \left(\{\nu_j\}_{j=1}^d \right).$$

Now since the eigenvalues of a Hermitian matrix majorize its diagonal elements by the Schur-Horn theorem [HJ13, Theorem 4.3.45],

$$\left\{ \mathbf{w}_j^\top \mathbf{K} \mathbf{w}_j \right\}_{j=1}^d \prec \{\nu_j\}_{j=1}^d.$$

Since ρ is Schur-concave, this implies

$$\rho \left(\left\{ \mathbf{w}_j^\top \mathbf{K} \mathbf{w}_j \right\}_{j=1}^d \right) \geq \rho \left(\{\nu_j\}_{j=1}^d \right) = \rho \left(\left\{ \tilde{\mathbf{w}}_j^\top \mathbf{K} \tilde{\mathbf{w}}_j \right\}_{j=1}^d \right).$$

Therefore, if ρ is Schur-concave, the rate constraint can only improve. This implies an optimal solution can be attained when \mathbf{W} is such that $\mathbf{W}^\top \mathbf{K} \mathbf{W}$ is diagonal. If ρ is strictly Schur-concave, the rate constraint strictly improves implying that the optimal \mathbf{W} must be such that $\mathbf{W}^\top \mathbf{K} \mathbf{W}$ is diagonal. This implies that

$$\begin{aligned} \text{tr} \left(\mathbf{K} \mathbf{W} \left(\mathbf{W}^\top \mathbf{K} \mathbf{W} + \sigma^2 \mathbf{I} \right)^{-1} \mathbf{W}^\top \mathbf{K} \right) &= \text{tr} \left(\mathbf{W}^\top \mathbf{K}^2 \mathbf{W} \left(\mathbf{W}^\top \mathbf{K} \mathbf{W} + \sigma^2 \mathbf{I} \right)^{-1} \right) \\ &= \sum_{i=1}^d \frac{\mathbf{w}_i^\top \mathbf{K}^2 \mathbf{w}_i}{\sigma^2 + \mathbf{w}_i^\top \mathbf{K} \mathbf{w}_i}. \end{aligned}$$

Note that minimizing the objective in (11) is equivalent to maximizing the above expression. Perform the change of variable

$$\begin{aligned} \mathbf{w}_j &\mapsto \begin{cases} \left(\frac{\mathbf{K}^{1/2}\mathbf{w}_j}{\|\mathbf{K}^{1/2}\mathbf{w}_j\|}, \|\mathbf{K}^{1/2}\mathbf{w}_j\|^2 \right) & \text{if } \mathbf{K}^{1/2}\mathbf{w}_j \neq \mathbf{0} \\ (0, 0) & \text{if } \mathbf{K}^{1/2}\mathbf{w}_j = \mathbf{0} \end{cases} \\ &= (\mathbf{y}_j, y_j). \end{aligned}$$

The assumption that $\mathbf{W}^\top \mathbf{K} \mathbf{W}$ is diagonal and the normalization in the definition of \mathbf{y}_j implies that

$$\mathbf{Y} = [\mathbf{y}_1 \mathbf{y}_2, \dots, \mathbf{y}_d]$$

is a matrix whose nonzero columns form an orthonormal set. Rewriting the objective in terms of the (\mathbf{y}_j, y_j) , we have

$$\sum_{i=1}^d \frac{\mathbf{w}_i^\top \mathbf{K}^2 \mathbf{w}_i}{\sigma^2 + \mathbf{w}_i^\top \mathbf{K} \mathbf{w}_i} = \sum_{i=1}^d \mathbf{y}_i^\top \mathbf{K} \mathbf{y}_i \frac{y_i}{\sigma^2 + y_i} = \sum_{i=1}^d \mathbf{y}_i^\top \mathbf{K} \mathbf{y}_i m_i, \quad (12)$$

where $m_i = \frac{y_i}{\sigma^2 + y_i}$. Observe that under this new parametrization, the constraint only depends on $\{y_i\}_{i=1}^d$. Without loss of generality, we assume that $y_1 \geq y_2 \geq \dots \geq y_d$, implying that $m_1 \geq m_2 \geq \dots \geq m_d$. We now prove that for given $\{y_i\}_{i=1}^d$, choosing the \mathbf{y}_i along the eigenvectors of \mathbf{K} is optimal.

Denote the diagonal elements of $\mathbf{Y}^\top \mathbf{K} \mathbf{Y}$ by $\{\lambda_i^2\}_{i=1}^d$ and let $\{\lambda_{i,\downarrow}^2\}_{i=1}^d$ denote the same diagonal elements arranged in descending order. Denote the eigenvalues of $\mathbf{Y}^\top \mathbf{K} \mathbf{Y}$ by $\{\mu_i^2\}_{i=1}^d$ where $\mu_1 \geq \mu_2 \geq \dots \geq \mu_d$. Again invoking the Schur-Horn theorem, the eigenvalues of $\mathbf{Y}^\top \mathbf{K} \mathbf{Y}$ majorize its diagonal entries

$$\{\lambda_i^2\}_{i=1}^d \prec \{\mu_i^2\}_{i=1}^d. \quad (13)$$

Substituting $\lambda_i^2 = \mathbf{y}_i^\top \mathbf{K} \mathbf{y}_i$ in (12), we have

$$\begin{aligned} \sum_{i=1}^d \lambda_i^2 m_i &\stackrel{(a)}{\leq} \sum_{i=1}^d \lambda_{i,\downarrow}^2 m_i = \lambda_{1,\downarrow}^2 m_1 + \sum_{i=2}^d \left(\sum_{j=1}^i \lambda_{j,\downarrow}^2 - \sum_{j=1}^{i-1} \lambda_{j,\downarrow}^2 \right) m_i \\ &= \lambda_{1,\downarrow}^2 m_1 + \sum_{i=2}^d m_i \sum_{j=1}^i \lambda_{j,\downarrow}^2 - \sum_{i=2}^d m_i \sum_{j=1}^{i-1} \lambda_{j,\downarrow}^2 \\ &= \lambda_{1,\downarrow}^2 (m_1 - m_2) + m_d \left(\sum_{j=1}^d \lambda_{j,\downarrow}^2 \right) + \sum_{i=2}^{d-1} (m_i - m_{i+1}) \sum_{j=1}^i \lambda_{j,\downarrow}^2 \\ &\stackrel{(b)}{\leq} \mu_1^2 (m_1 - m_2) + m_d \left(\sum_{j=1}^d \mu_j^2 \right) + \sum_{i=2}^{d-1} (m_i - m_{i+1}) \sum_{j=1}^i \mu_j^2 \\ &\stackrel{(c)}{\leq} \sigma_1^2 (m_1 - m_2) + m_d \left(\sum_{j=1}^d \sigma_j^2 \right) + \sum_{i=2}^{d-1} (m_i - m_{i+1}) \sum_{j=1}^i \sigma_j^2 \\ &= \sum_{i=1}^d \sigma_i^2 m_i, \end{aligned}$$

where inequality (a) follows from the assumption that $m_1 \geq m_2 \geq \dots \geq m_d$, and (b) from the definition in (13). Since \mathbf{Y} 's nonzero columns form an orthonormal set, the eigenvalues of $\mathbf{Y}^\top \mathbf{K} \mathbf{Y}$, when arranged in descending order, are at most the eigenvalues of \mathbf{K} from Corollary 4.3.37 in [HJ13], and therefore (c) follows.

This upper bound is attained when $\mathbf{y}_i = \mathbf{u}_i$ for nonzero y_i , where \mathbf{u}_i is the normalized eigenvector of \mathbf{K} corresponding to eigenvalue σ_i^2 . To see this, note that when $\mathbf{y}_i = \mathbf{u}_i$, $\lambda_i^2 = \mu_i^2 = \sigma_i^2$. From the definition of \mathbf{y}_i , $\mathbf{w}_i = \mathbf{K}^{-1/2} \mathbf{u}_i \sqrt{y_i} = \mathbf{u}_i \frac{\sqrt{y_i}}{\sigma_i}$. Therefore, for a Schur-concave ρ , the set of matrices whose nonzero columns are eigenvectors of \mathbf{K} is optimal. We now prove that for a strictly Schur-concave ρ , if \mathbf{K} has distinct eigenvalues, this set contains all of the optimal solutions \mathbf{W} .

We know that for a fixed $y_1 \geq y_2 \geq \dots \geq y_d$, (implying a fixed $m_1 \geq m_2 \geq \dots \geq m_d$) the upper bound $\sum_{i=1}^d \sigma_i^2 m_i$ is attained by the previous choice of \mathbf{y}_i . Note that if all nonzero m_i are distinct, equality in (b) and (c) is attained if and only if the nonzero diagonal elements of $\mathbf{Y}^\top \mathbf{K} \mathbf{Y}$ equal the corresponding eigenvalues of \mathbf{K} . This implies that, if all nonzero m_i are distinct, the upper bound is attained if and only if $\mathbf{y}_i = \mathbf{u}_i$ for nonzero y_i . Therefore, it is sufficient to prove that for the following optimization problem

$$\begin{aligned} & \sup_{\{y_i \geq 0\}} \sum_{i=1}^d \sigma_i^2 \frac{y_i}{\sigma^2 + y_i} \\ & \text{subject to } R \geq \rho \left(\{y_i\}_{i=1}^d \right), \end{aligned} \quad (14)$$

any optimal $\{y_i\}$ must be such that the nonzero y_i are distinct. Firstly, note that since $\sigma_1^2 > \sigma_2^2 > \dots > \sigma_d^2$, we must have $y_1 \geq y_2 \geq \dots \geq y_d$. Assume to the contrary that for an optimal $\{y_i\}_{i=1}^d$ there exists $1 \leq j, \ell < d$ such that $y_{j-1} > y_j = y_{j+1} = y_{j+2} = \dots = y_{j+\ell} > y_{j+\ell+1} \geq 0$, where y_0 is chosen to be any real number strictly greater than y_1 and $y_{d+1} = 0$. Take $\delta > 0$ small. Denote a new sequence $\{y'_i\}_{i=1}^d$ where $y'_j = y_j + \delta$, $y'_{j+\ell} = y_{j+\ell} - \delta$ and $y'_i = y_i$ for $1 \leq i \leq d$ with $i \neq j$ and $j + \ell$. Since ρ is strictly Schur-concave, the constraint is strictly improved,

$$\rho \left(\{y'_i\}_{i=1}^d \right) < \rho \left(\{y_i\}_{i=1}^d \right).$$

Since $\sigma_j^2 > \sigma_{j+\ell}^2$, the objective is strictly improved for sufficiently small δ ,

$$\sum_{i=1}^d \sigma_i^2 \frac{y_i}{\sigma^2 + y_i} < \sum_{i=1}^d \sigma_i^2 \frac{y'_i}{\sigma^2 + y'_i},$$

as desired. \square

As a consequence of Theorem 1, encoding via an optimal \mathbf{W} can be viewed as a projection along the eigenvectors of \mathbf{K} , followed by different scalings applied to each component, i.e. $\mathbf{W} = \mathbf{U} \mathbf{S}$ where \mathbf{S} is a diagonal matrix with entries $s_i \geq 0$ and \mathbf{U} is the normalized eigenvector matrix. Only \mathbf{S} remains to be determined, and to this end, we may assume that \mathbf{K} is diagonal with nonincreasing diagonal entries, implying $\mathbf{U} = \mathbf{I}$. In subsequent sections, our choice of ρ will be

of the form $\sum_{i=1}^d \rho_{sl}$, where $\rho_{sl} : \mathbb{R}_{\geq 0} \rightarrow \mathbb{R}_{\geq 0}$ ¹ is (strictly) concave, making ρ (strictly) Schur-concave (see Proposition 9 in Appendix A). Therefore, (11) reduces to

$$\begin{aligned} \inf_{\mathbf{S}} \quad & \text{tr}(\mathbf{K}) - \text{tr}(\mathbf{K}\mathbf{S}(\mathbf{S}^\top \mathbf{K}\mathbf{S} + \sigma^2 \mathbf{I})^{-1} \mathbf{S}^\top \mathbf{K}) \\ \text{subject to} \quad & R \geq \rho_{sl}(\{s_i^2 \sigma_i^2\}), \end{aligned} \quad (15)$$

where the infimum is over diagonal matrices \mathbf{S} . To handle situations for which

$$\lim_{s \rightarrow \infty} \rho_{sl}(s) < \infty, \quad (16)$$

we allow the diagonal entries of \mathbf{S} to be ∞ , with the objective for such cases defined via its continuous extension.

In the next section, we will solve (15) for several specific choices of ρ_{sl} .

3 Explicit Solutions: Conventional Linear Autoencoders and PBA

3.1 Conventional Linear Autoencoders

Given a centered dataset $\mathbf{x}_1, \mathbf{x}_2, \dots, \mathbf{x}_n \in \mathbb{R}^d$, consider a linear autoencoder optimization problem where the encoder and decoder, \mathbf{W} and \mathbf{T} , respectively, are d -by- k matrices where $k \leq d$ is a parameter. The goal is to minimize the mean squared error as given by (5). PCA corresponds to the global optimal solution of this optimization problem, where $\mathbf{W} = \mathbf{T} = \mathbf{U}_k$, where $\mathbf{U}_k \in \mathbb{R}^{d \times k}$ is a matrix whose columns are the k eigenvectors corresponding to the k largest eigenvalues of \mathbf{K} . However, there are multiple global optimal solutions, given by any encoder-decoder pair of the form $(\mathbf{U}_k \mathbf{V}, \mathbf{U}_k \mathbf{V})$, where \mathbf{V} is an orthogonal matrix [BH89].

We now recover linear autoencoders through our framework in Section 2. Consider the optimization problem in (15) where $\rho_{sl} : \mathbb{R}_{\geq 0} \rightarrow \{0, 1\}$ is a concave function defined as

$$\rho_{sl}(x) = \mathbf{1}[x > 0]. \quad (17)$$

Note that this penalizes the dimension of the latents, as desired. Note also that this cost is Schur-concave but not strictly so. The fact that PCA solves conventional linear autoencoding, but is not necessarily the unique solution, follows immediately from Theorem 1.

Theorem 2. *If $\rho_{sl}(\cdot)$ is given by (17), then an optimal solution for (15) is given by a diagonal matrix \mathbf{S} whose top $\min(\lfloor R \rfloor, d)$ diagonal entries are equal to ∞ and the remaining entries are 0.*

Proof. Let $\mathcal{F} \stackrel{\text{def}}{=} \{i \in [d] : s_i > 0\}$, implying $|\mathcal{F}| \leq R$. Since \mathbf{K} and \mathbf{S} are diagonal, the optimization problem in (15) can be written as

$$\begin{aligned} \inf_{\{s_\ell\}} \quad & \sum_{j \in [d] \setminus \mathcal{F}} \sigma_j^2 + \sum_{\ell \in \mathcal{F}} \frac{\sigma^2 \sigma_\ell^2}{\sigma^2 + \sigma_\ell^2 s_\ell^2} \\ \text{subject to} \quad & R \geq \sum_{i=1}^d \mathbf{1}[s_i > 0]. \end{aligned} \quad (18)$$

¹“sl” stands for single-letter

Since the value of $s_\ell, \ell \in \mathcal{F}$ does not affect the rate constraint, each of the s_ℓ can be made as large as possible without changing the rate constraint. Therefore, the infimum value of the objective is $\sum_{j \in [d] \setminus \mathcal{F}} \sigma_j^2$. Since we seek to minimize the distortion, the optimal \mathcal{F} is the set of indices with the largest $|\mathcal{F}|$ eigenvalues. Since the number of these eigenvalues cannot exceed R , we choose $|\mathcal{F}| = \min(\lfloor R \rfloor, d)$. \square

Unlike the conventional linear autoencoder framework, in Section 2, the latent variables $\mathbf{W}^\top \mathbf{x}$ are quantized, which we model with additive white noise of fixed variance. Therefore, an infinite value of s_i indicates sending $\mathbf{u}_i^\top \mathbf{x}$ with full precision where \mathbf{u}_i is the eigenvector corresponding to the i^{th} largest eigenvalue. This implies that PCA with parameter k corresponds to $\mathbf{W} = \mathbf{U}\mathbf{S}$, where \mathbf{S} is a diagonal matrix whose top k diagonal entries are equal to ∞ and the $d - k$ remaining diagonal entries are 0. Therefore, for any R such that $\lfloor R \rfloor = k$, an optimal solution to (15) corresponds to linearly projecting the data along the top k eigenvectors, which is the same as PCA. Note that, like [BH89], we only prove that projecting along the eigenvectors is one of possibly other optimal solutions. However, even a slight amount of curvature in ρ would make it strictly Schur-concave, thus recovering the principal directions. We next turn to a specific cost function with curvature, namely the PBA cost function that was our original motivation.

3.2 Principal Bit Analysis (PBA)

Consider the choice of $\rho_{sl} : \mathbb{R}_{\geq 0} \rightarrow \mathbb{R}_{\geq 0}$ that provided the original impetus for Theorem 1. For $\gamma > \frac{2}{\sigma^2}$,

$$\rho_{sl}(x) = \frac{1}{2} \log(\gamma x + 1). \quad (19)$$

The nature of the optimization problem depends on the value of γ . For $1 \leq \gamma\sigma^2 \leq 2$, the problem can be made convex with a simple change of variable. For $\gamma\sigma^2 = 1$, the problem coincides with the classical waterfilling procedure in rate-distortion theory, in fact. For $\gamma\sigma^2 > 2$, the problem is significantly more challenging. Since we are interested in relatively large values of γ for our compression application (see Section 5 to follow), we focus on the case $\gamma > 2/\sigma^2$.

Theorem 3. *If $\rho_{sl}(\cdot)$ is given by (19) for $\gamma > \frac{2}{\sigma^2}$, then for any $\lambda > 0$, the pair $\bar{R}_{opt}, \bar{D}_{opt}$ obtained from the output of Algorithm 1 satisfies*

$$\bar{D}_{opt} + \lambda \bar{R}_{opt} = \inf_{\mathbf{S}} \left[\text{tr}(\mathbf{K}) - \text{tr}(\mathbf{K}\mathbf{S}(\mathbf{S}^\top \mathbf{K}\mathbf{S} + \sigma^2 \mathbf{I})^{-1} \mathbf{S}^\top \mathbf{K}) + \lambda \sum_{i=1}^d \rho_{sl}(\{s_i^2 \sigma_i^2\}) \right], \quad (21)$$

Proof. Since \mathbf{K} and \mathbf{S} are diagonal, the optimization problem in (21) can be written as

$$\inf_{\{s_i\}} \sum_{i=1}^d \frac{\sigma_i^2 \sigma_i^2}{\sigma^2 + s_i^2 \sigma_i^2} + \lambda \cdot \frac{1}{2} \sum_{i=1}^d \log(1 + \gamma s_i^2 \sigma_i^2). \quad (22)$$

With the following change of variables $\alpha = \gamma\sigma^2$, $s_i \mapsto s_i'^2 = \alpha \frac{s_i^2}{\sigma^2}$, we obtain

$$\inf_{\{s_i'\}} \sum_{i=1}^d \frac{\sigma_i^2}{\alpha + s_i'^2 \sigma_i^2} + \lambda \cdot \frac{1}{2} \sum_{i=1}^d \log(1 + s_i'^2 \sigma_i^2). \quad (23)$$

Algorithm 1 Principal Bit Analysis (PBA)

Require: $\lambda > 0, \alpha > 2$,

$$\mathbf{K} = \begin{bmatrix} \sigma_1^2 & 0 & \cdots & 0 \\ 0 & \sigma_2^2 & \cdots & 0 \\ \vdots & \vdots & \ddots & \vdots \\ 0 & 0 & \cdots & \sigma_d^2 \end{bmatrix} \succ 0, \quad (20)$$

such that $\sigma_1^2 \geq \sigma_2^2 \geq \cdots \geq \sigma_d^2$.

- 1: If $\lambda \geq \sigma_1^2/(4(\alpha - 1))$, Output $\bar{R}_{\text{opt}} = 0, \bar{D}_{\text{opt}} = \sum_{i=1}^d \sigma_i^2$.
 - 2: Set $\bar{d} = \max \{i : \lambda < \sigma_i^2/4(\alpha - 1)\}$.
 - 3: Set \bar{R}, \bar{D} to zero arrays of size $2\bar{d}$.
 - 4: **for** $r \in \{1, 2, \dots, \bar{d}\}$ **do**
 - 5: $\bar{D}(2r - 1) = \sum_{i=1}^r \frac{\sigma_i^2}{2(\alpha-1)} \left(1 - \sqrt{1 - \frac{4\lambda(\alpha-1)}{\sigma_i^2}}\right) + \sum_{i=r+1}^d \frac{\sigma_i^2}{\alpha}$,
 - 6: $\bar{R}(2r - 1) = \sum_{i=1}^r \frac{1}{2} \log \left(\frac{\sigma_i^2}{4\lambda}\right) + \log \left(1 + \sqrt{1 - \frac{4\lambda(\alpha-1)}{\sigma_i^2}}\right)$.
 - 7: $\bar{D}(2r) = \left(\sum_{i=1}^{r-1} \frac{\sigma_i^2}{2(\alpha-1)} \left(1 - \sqrt{1 - \frac{4\lambda(\alpha-1)}{\sigma_i^2}}\right) + \frac{\sigma_r^2}{2(\alpha-1)} \left(1 + \sqrt{1 - \frac{4\lambda(\alpha-1)}{\sigma_r^2}}\right) + \sum_{i=r+1}^d \frac{\sigma_i^2}{\alpha}\right)$.
 - 8: $\bar{R}(2r) = \sum_{i=1}^r \frac{1}{2} \log \left(\frac{\sigma_i^2}{4\lambda}\right) + \sum_{i=1}^{r-1} \log \left(1 + \sqrt{1 - \frac{4\lambda(\alpha-1)}{\sigma_i^2}}\right) + \log \left(1 - \sqrt{1 - \frac{4\lambda(\alpha-1)}{\sigma_r^2}}\right)$.
 - 9: **end for**
 - 10: $r^* \leftarrow \arg \min_{j \in [2\bar{d}]} \bar{D}(j) + \lambda \bar{R}(j)$.
 - 11: Output $\bar{R}_{\text{opt}} = \bar{R}(r^*), \bar{D}_{\text{opt}} = \bar{D}(r^*)$.
-

Ignoring the constant factor in the objective, perform the change of variable $s'_i \mapsto D_i = \frac{\sigma_i^2}{\alpha + s_i'^2 \sigma_i^2}$ to obtain

$$\begin{aligned} \inf_{\{D_i\}} \quad & \sum_{i=1}^d D_i + \frac{\lambda}{2} \sum_{i=1}^d \log \left(\frac{\sigma_i^2}{D_i} - (\alpha - 1) \right), \\ \text{subject to} \quad & D_i \leq \frac{\sigma_i^2}{\alpha} \quad \text{for all } i \in [d]. \end{aligned} \quad (24)$$

This optimization problem is nonconvex since the function $\log \left(\frac{\sigma_i^2}{D_i} - (\alpha - 1) \right)$ is convex for $0 \leq D_i \leq \frac{\sigma_i^2}{2(\alpha-1)}$ but concave for $\frac{\sigma_i^2}{2(\alpha-1)} < D_i \leq \frac{\sigma_i^2}{\alpha}$ and the latter interval is nonempty since $\alpha > 2$.

Any optimizing $\{D_i\}$ must be a stationary point of

$$\mathcal{L} \left(\{D_i\}_{i=1}^d, \lambda, \{\mu_i\}_{i=1}^d \right) = \sum_{i=1}^d D_i + \lambda \left(\sum_{i=1}^d \log \left(\frac{\sigma_i^2}{D_i} - (\alpha - 1) \right) \right) + \sum_{i=1}^d \mu_i \left(D_i - \frac{\sigma_i^2}{\alpha} \right). \quad (25)$$

for some $\{\mu_i\}_{i=1}^d$ with $\mu_i \geq 0$ for all $i \in [d]$ and satisfying the complementary slackness condi-

tion [Ber99, Prop. 3.3.1]. The stationary points satisfy, for each i

$$\frac{\partial \mathcal{L}}{\partial D_i} = 1 - \lambda \left(\frac{\frac{\sigma_i^2}{D_i^2}}{\left(\frac{\sigma_i^2}{D_i} - (\alpha - 1) \right)} \right) + \mu_i = 0. \quad (26)$$

Let $\mathcal{F} = \left\{ i : D_i < \frac{\sigma_i^2}{\alpha} \right\}$. For $i \in \mathcal{F}$, $\mu_i = 0$ due to complementary slackness. Substituting in (26) we obtain a quadratic equation in D_i

$$(\alpha - 1)D_i^2 - \sigma_i^2 D_i + \lambda \sigma_i^2 = 0.$$

which gives

$$D_i = \frac{\sigma_i^2}{2(\alpha - 1)} \left(1 \pm \sqrt{1 - \frac{4\lambda(\alpha - 1)}{\sigma_i^2}} \right).$$

Let $c_i = \sqrt{1 - \frac{4\lambda(\alpha - 1)}{\sigma_i^2}}$. Note that $\frac{\sigma_i^2}{2(\alpha - 1)} (1 + c_i)$ is always in the concave region and $\frac{\sigma_i^2}{2(\alpha - 1)} (1 - c_i)$ is always in the convex region for a λ chosen such that D_i is a real number strictly less than $\frac{\sigma_i^2}{\alpha}$.

Therefore the optimal set of distortions are contained in the following set of 3^d points

$$\prod_{i=1}^d \left\{ \frac{\sigma_i^2}{2(\alpha - 1)} \left(1 + \sqrt{1 - \frac{4\lambda(\alpha - 1)}{\sigma_i^2}} \right), \frac{\sigma_i^2}{2(\alpha - 1)} \left(1 - \sqrt{1 - \frac{4\lambda(\alpha - 1)}{\sigma_i^2}} \right), \frac{\sigma_i^2}{\alpha} \right\}.$$

We now reduce the size of the above set by making a two observations:

(1). \mathcal{F} is contiguous.

Lemma 4. *There exists an optimal $\{D_i^*\}_{i=1}^d$ for (24) such that (a) $\frac{\sigma_i^2}{D_i^*}$ is a nonincreasing sequence and (b) $\mathcal{F} = \{1, 2, \dots, |\mathcal{F}|\}$.*

Proof. Substitute $x_i = \frac{\sigma_i^2}{D_i}$ in (24). This gives us

$$\begin{aligned} \inf_{\{x_i\}} \quad & \sum_{i=1}^d \frac{\sigma_i^2}{x_i} + \frac{\lambda}{2} \sum_{i=1}^d \log(x_i - (\alpha - 1)), \\ \text{subject to} \quad & x_i \geq \alpha \quad \text{for all } i \in [d]. \end{aligned} \quad (27)$$

Let $\{x_i^*\}_{i=1}^d$ be an optimal solution for (27). If, for $i > j$, $x_i^* > x_j^* \geq \alpha$, then exchanging the values provides a solution that has the same rate and lower distortion since $\frac{\sigma_i^2}{x_i^*} + \frac{\sigma_j^2}{x_j^*} \geq \frac{\sigma_i^2}{x_j^*} + \frac{\sigma_j^2}{x_i^*}$. This proves (a). Part (b) follows immediately. \square

(2). No two solutions are concave.

Lemma 5. *For $R > 0$, let $\{D_i^*\}_{i=1}^d$ be an optimal solution for (24). There exists at most one D_i^* such that $\frac{\sigma_i^2}{2(\alpha - 1)} < D_i^* < \frac{\sigma_i^2}{\alpha}$.*

Proof. Let D_i^*, D_j^* be such that $\frac{\sigma_i^2}{2(\alpha-1)} < D_i^* < \frac{\sigma_i^2}{\alpha}$ and $\frac{\sigma_j^2}{2(\alpha-1)} < D_j^* < \frac{\sigma_j^2}{\alpha}$. Without loss of generality, assume $D_i^* < D_j^*$. Denote the individual rate constraint function by $r(D_i) \triangleq \log\left(\frac{\sigma_i^2}{D_i} - (\alpha-1)\right)$. Since r is concave in $\left(\frac{\sigma_i^2}{2(\alpha-1)}, \frac{\sigma_i^2}{\alpha}\right)$, there exist an $\varepsilon > 0$ such that

$$r(D_i^* - \varepsilon) + r(D_j^* + \varepsilon) = r(D_i^*) - \varepsilon r'(D_i^*) + O(\varepsilon^2) + r(D_j^*) + \varepsilon r'(D_j^*) + O(\varepsilon^2) \quad (28)$$

$$< r(D_i^*) + r(D_j^*) \quad (29)$$

The last inequality follows from concavity of r . Therefore, replacing (D_i^*, D_j^*) with $(D_i^* - \varepsilon, D_j^* + \varepsilon)$, the rate constraint can be improved while keeping the objective in (24) constant, contradicting the optimality assumption of $\{D_i^*\}$. \square

There is at most one D_i^* such that $D_i^* = \frac{\sigma_i^2}{2(\alpha-1)}(1+c_i)$. Assuming such an i exists, $x_i = \frac{2(\alpha-1)}{1+c_i} < 2(\alpha-1)$. For the convex roots, $x_i = \frac{2(\alpha-1)}{1-c_i} > 2(\alpha-1)$. Therefore from Lemma 4, all the convex roots are contiguous. Therefore, the set of potentially optimal solutions reduces to cardinality $2d$, where each solution is characterized by the number of components that send non-zero rate and whether or not a concave root is sent. PBA, detailed in Algorithm 1 finds the minimum value of the Lagrangian across these $2d$ solutions for a fixed λ . \square

Note that by sweeping $\lambda > 0$, one can compute the lower convex envelope of the (D, R) curve. Since every Pareto optimal (D, R) must be a stationary point of (21), one can also use Algorithm 1 to compute the (D, R) curve itself by sweeping λ and retaining all those stationary points that are not Pareto dominated.

4 Application to Variable-Rate Compression

We have seen that an autoencoder formulation inspired by data compression succeeds in providing guaranteed recovery the principal source components. Conversely, a number of successful multimedia compressors have recently been proposed that are either related to, or directly inspired by, autoencoders [TAL18, TVJ⁺17, BLS16, TOH⁺16, TSCH17, RB17, HRTC19, AMT⁺17, BMS⁺18, ZCG⁺18, ATM⁺19, BCM⁺20]. In particular, Ballé *et al.* [BMS⁺18] show that the objective minimized by their compressor coincides with that of variational autoencoders. Following [BCM⁺20], we refer to this objective as *nonlinear transform coding (NTC)*. We next use Theorem 1 to show that any minimizer of the NTC objective is guaranteed to recover the principal source components if (1) the source is Gaussian, (2) the transforms are restricted to be linear, and (3) the entropy model is *factorized*, as explained below.

Let $\mathbf{x} \sim \mathcal{N}(0, \mathbf{K})$, where \mathbf{K} is a positive semidefinite covariance matrix. As before, we consider an autoencoder defined by its encoder-decoder pair (f, g) , where for $k \leq d$, $f: \mathbb{R}^d \rightarrow \mathbb{R}^k$ and $g: \mathbb{R}^k \rightarrow \mathbb{R}^d$ are chosen from prespecified classes \mathcal{C}_f and \mathcal{C}_g . The NTC framework assumes dithered quantization during training, as in Section 2 and [AT20, CEKL19], and seeks to minimize the Lagrangian

$$\inf_{f \in \mathcal{C}_f, g \in \mathcal{C}_g} \mathbb{E}_{\mathbf{x}, \varepsilon} \left[\|\mathbf{x} - g(Q(f(\mathbf{x}) + \varepsilon) - \varepsilon)\|_2^2 \right] + \lambda H(Q(f(\mathbf{x}) + \varepsilon) - \varepsilon | \varepsilon). \quad (30)$$

where $\lambda > 0$ and ε has i.i.d. $\text{Unif}[-0.5, 0.5]$ components. NTC assumes variable-length compression, and the quantity

$$H(Q(f(x) + \varepsilon) - \varepsilon | \varepsilon)$$

is an accurate estimate of minimum expected codelength length for the discrete random vector $Q(f(x) + \varepsilon)$. As we noted in Section 2, [ZF92] showed that for any random variable x , $Q(x + \varepsilon) - \varepsilon$ and $x + \varepsilon$ have the same joint distribution with x . They also showed that $H(Q(x + \varepsilon) - \varepsilon | \varepsilon) = I(x + \varepsilon; x) = h(x + \varepsilon)$, where $h(\cdot)$ denotes differential entropy. Therefore, the objective can be written as

$$\inf_{f \in \mathcal{C}_f, g \in \mathcal{C}_g} \mathbb{E}_{x, \varepsilon} \left[\|x - g(f(x) + \varepsilon)\|_2^2 \right] + \lambda h(f(x) + \varepsilon). \quad (31)$$

(Compare eq.(13) in [BCM⁺20]).

We consider the case in which $\mathcal{C}_f, \mathcal{C}_g$ are the class of linear functions. Let \mathbf{W}, \mathbf{T} be d -by- d matrices. Define $f(x) = \mathbf{W}^\top x$, $g(x) = \mathbf{T}x$. Substituting this in the above equation, we obtain

$$\inf_{\mathbf{W}, \mathbf{T}} \mathbb{E}_{x, \varepsilon} \left[\left\| x - \mathbf{T} \left(\mathbf{W}^\top x + \varepsilon \right) \right\|_2^2 \right] + \lambda h(\mathbf{W}^\top x + \varepsilon). \quad (32)$$

Since \mathbf{T} does not appear in the rate constraint, the optimal \mathbf{T} can be chosen to be the minimum mean squared error estimator of $x \sim \mathcal{N}(0, \mathbf{K})$ given $\mathbf{W}^\top x + \varepsilon$, as in Section 2. This gives

$$\inf_{\mathbf{W}} \text{tr}(\mathbf{K}) - \text{tr}(\mathbf{K} \mathbf{W} \left(\mathbf{W}^\top \mathbf{K} \mathbf{W} + \frac{\mathbf{I}}{12} \right)^{-1} \mathbf{W}^\top \mathbf{K}) + \lambda h(\mathbf{W}^\top x + \varepsilon). \quad (33)$$

As noted earlier, the rate term $h(\mathbf{W}^\top x + \varepsilon)$ is an accurate estimate for the minimum expected length of the compressed representation of $Q(\mathbf{W}^\top x + \varepsilon)$. This assumes that the different components of this vector are encoded jointly, however. In practice, one often encodes them separately, relying on the transform \mathbf{W} to eliminate redundancy among the components. Accordingly, we replace the rate term with

$$\sum_{i=1}^d h(\mathbf{w}_i^\top x + [\varepsilon]_i),$$

to arrive at the optimization problem

$$\inf_{\mathbf{W}} \text{tr}(\mathbf{K}) - \text{tr}(\mathbf{K} \mathbf{W} \left(\mathbf{W}^\top \mathbf{K} \mathbf{W} + \frac{\mathbf{I}}{12} \right)^{-1} \mathbf{W}^\top \mathbf{K}) + \lambda \cdot \sum_{i=1}^d h(\mathbf{w}_i^\top x + [\varepsilon]_i). \quad (34)$$

Theorem 6. *Suppose \mathbf{K} has distinct eigenvalues. Then any \mathbf{W} that achieves the infimum in (34) has the property that all of its nonzero rows are eigenvectors of \mathbf{K} .*

Proof. Since the distribution of ε is fixed, by the Gaussian assumption on x , $h(\mathbf{w}_j^\top x + [\varepsilon]_j)$ only depends on \mathbf{w}_j through $\mathbf{w}_j^\top \mathbf{K} \mathbf{w}_j$. Thus we may write

$$h(\mathbf{w}_j^\top x + \varepsilon) = \rho_{sl}(\mathbf{w}_j^\top \mathbf{K} \mathbf{w}_j). \quad (35)$$

By Theorem 1, it suffices to show that $\rho_{sl}(\cdot)$ is strictly concave. Let Z be a standard Normal random variable and let ϵ be uniformly distributed over $[-1/2, 1/2]$, independent of Z . Then we have

$$\rho_{sl}(s) = h(\sqrt{s} \cdot Z + \epsilon). \quad (36)$$

Thus by de Bruijn's identity [CT06],

$$\rho'_{sl}(s) = \frac{1}{2}J(\epsilon + \sqrt{s} \cdot Z), \quad (37)$$

where $J(\cdot)$ is the Fisher information. To show that $\rho'_{sl}(\cdot)$ is strictly concave, it suffices to show that $J(\epsilon + \sqrt{s} \cdot Z)$ is strictly decreasing in s .² To this end, let $t > s > 0$ and let Z_1 and Z_2 be i.i.d. standard Normal random variables, independent of ϵ . Then

$$J(\epsilon + \sqrt{t} \cdot Z) = J(\epsilon + \sqrt{s} \cdot Z_1 + \sqrt{t-s} \cdot Z_2) \quad (38)$$

and by the convolution inequality for Fisher information [Bla65],

$$\frac{1}{J(\epsilon + \sqrt{s} \cdot Z_1 + \sqrt{t-s} \cdot Z_2)} > \frac{1}{J(\epsilon + \sqrt{s} \cdot Z_1)} + \frac{1}{J(\sqrt{t-s} \cdot Z_2)} > \frac{1}{J(\epsilon + \sqrt{s} \cdot Z_1)}, \quad (39)$$

where the first inequality is strict because $\epsilon + \sqrt{s} \cdot Z_1$ is not Gaussian distributed. \square

5 Compression Experiments

We validate the PBA algorithm experimentally by comparing the performance of a PBA-derived fixed-rate compressor against the performance of baseline fixed-rate compressors. The code of our implementation can be found at <https://github.com/SourbhBh/PBA>. As we noted in the previous section, although variable-rate codes are more commonplace in practice, fixed-rate codes do offer some advantages over their more general counterparts:

1. In applications where a train of source realizations are compressed sequentially, fixed-rate coding allows for simple concatenation of the compressed representations. Maintaining synchrony between the encoder and decoder is simpler than with variable-rate codes.
2. In applications where a dataset of source realizations are individually compressed, fixed-rate coding allows for random access of data points from the compressed representation.
3. In streaming in which a sequence of realizations will be streamed, bandwidth provisioning is simplified when the bit-rate is constant over time.

Fixed-rate compressors exist for specialized sources such as speech [MB95, SA85] and audio more generally [Vor]. We consider a general-purpose, learned, fixed-rate compressor derived from PBA and the following two quantization operations. The first, $Q_{CD}(a, \sigma^2, U, x)$ ³ accepts the

²If $g'(\cdot)$ is strictly decreasing then for all $t > s$, $g(t) = g(s) + \int_s^t g'(u)du < g(s) + g'(s)(t-s)$ and likewise for $t < s$. That $g(\cdot)$ is strictly concave then follows from the standard first-order test for concavity [BV04].

³“CD” stands for “clamped dithered.”

hyperparameter a , a variance estimate σ^2 , a dither realization U , and the scalar source realization to be compressed, x , and outputs (a binary representation of) the nearest point to x in the set

$$\left\{ i + U : i \in \mathbb{Z} \text{ and } i + U \in \left(-\frac{\Gamma}{2}, \frac{\Gamma}{2} \right] \right\}, \quad (40)$$

where

$$\Gamma = 2^{\lfloor \frac{1}{2} \log_2(4a^2\sigma^2+1) \rfloor}. \quad (41)$$

This evidently requires $\log_2 \Gamma$ bits. The second function, $Q'_{CD}(a^2, \sigma^2, U, b)$, where b is a binary string of length $\log_2 \Gamma$, maps the binary representation b to the point in (40). These quantization routines are applied separately to each latent component. The σ^2 parameters are determined during training. The dither U is chosen uniformly over the set $[-1/2, 1/2]$, independently for each component. We assume that U is chosen pseudorandomly from a fixed seed that is known to both the encoder and the decoder. As such, it does not need to be explicitly communicated. For our experiments, we fix the a parameter at 15 and hard code this both at the encoder and at the decoder. We found that this choice balances the dual goals of minimizing the excess distortion due to the clamping quantized points to the interval $(\Gamma/2, \Gamma/2]$ and minimizing the rate.

PBA compression proceeds by applying Algorithm 1 to a training set to determine the matrices \mathbf{W} and \mathbf{T} . The variance estimates $\sigma_1^2, \dots, \sigma_d^2$ for the d latent variances are chosen as the empirical variances on the training set and are hard-coded in the encoder and decoder. Given a data point x , the encoded representation is the concatenation of the bit strings b_1, \dots, b_d , where

$$b_i = Q_{CD}(a^2, \sigma_i^2, U_i, \mathbf{w}_i^\top x),$$

The decoder parses the received bits into b_1, \dots, b_d . and computes the latent reconstruction $\hat{\mathbf{y}}$, where

$$\hat{\mathbf{y}}_i = Q'_{CD}(a^2, \sigma_i^2, U_i, b_i),$$

The reconstruction is then $\mathbf{T}\hat{\mathbf{y}}$.

We evaluate the PBA compressor on MNIST [LBBH98], CIFAR-10 [Kri09], MIT Faces Dataset, Free Spoken Digit Dataset (FSDD) [Jac] and a synthetic Gaussian dataset. The synthetic Gaussian dataset is generated from a diagonal covariance matrix obtained from the eigenvalues of the Faces Dataset. We compare our algorithms primarily using mean-squared error since our theoretical analysis uses mean squared error as the distortion metric. Our plots display Signal-to-Noise ratios (SNRs) for ease of interpretation. For image datasets, we also compare our algorithms using the Structural Similarity (SSIM) or the Multi-scale Structural Similarity (MS-SSIM) metrics when applicable [WBSS04]. We also consider errors on downstream tasks, specifically classification, as a distortion measure.

For all datasets, we compare the performance of the PBA compressor against baseline scheme derived from PCA that uses Q_{CD} and Q'_{CD} . The PCA-based scheme sends some of the principal components essentially losslessly, and no information about the others. Specifically, in the context of our framework, for any given k , we choose the first k columns of \mathbf{W} to be aligned with the first k principal components of the dataset; the remaining columns are zero. Each nonzero column is scaled such that its Euclidean length multiplied by the eigenvalue has all the significant digits. This is done so that at high rates, the quantization procedure sends the k principal components losslessly. The quantization and decoder operations are as in the PBA-based scheme; in particular the a^2 parameter is as specified above. By varying k , we trade off rate and distortion.

5.1 SNR Performance

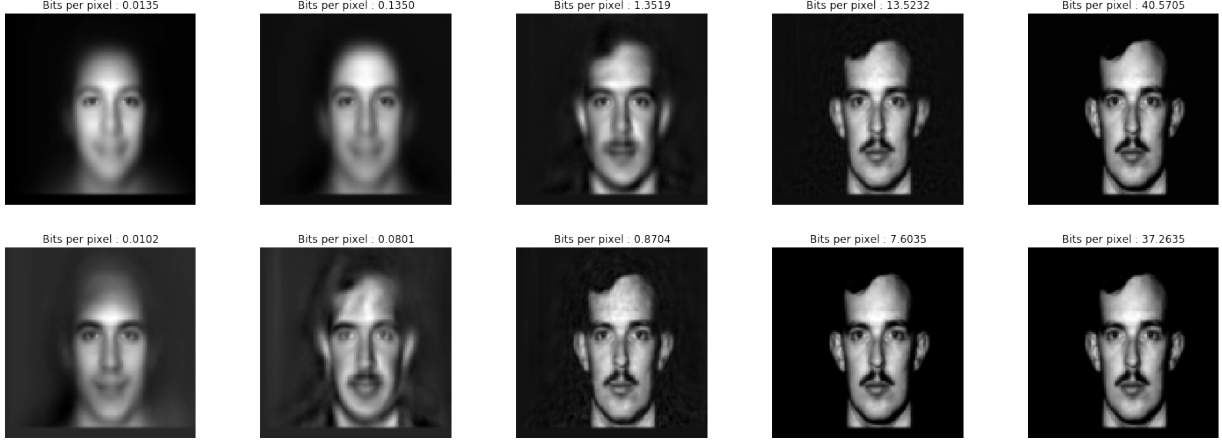


Figure 2: Reconstructions at different bits/pixel values for PCA (top) and PBA (bottom)

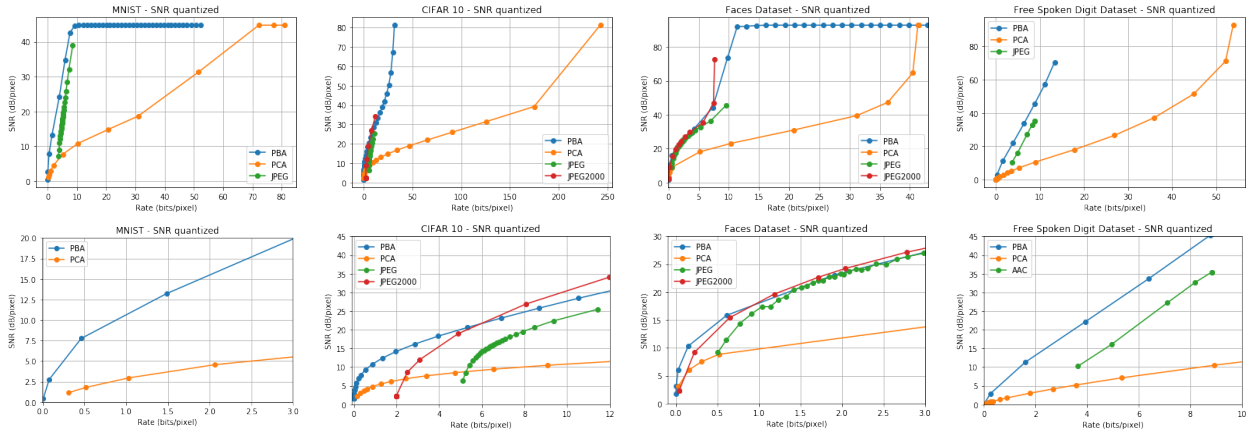


Figure 3: SNR/pixel vs Rate (bits/pixel) for MNIST, CIFAR-10, Faces, FSDD datasets. Figures in the bottom row are zoomed-in.

We begin by examining compression performance under mean squared error, or equivalently, the SNR, defined as

$$\text{SNR} = 10 \cdot \log_{10} \left(\frac{P}{\text{MSE}} \right).$$

where P is the empirical second moment of the dataset. This was the objective that PBA (and PCA) is designed to minimize.

In Figure 2, we display reconstructions for a particular image in the Faces Dataset under PBA and PCA. Figure 3 shows the tradeoff for PBA and PCA against JPEG and JPEG2000 (for the image datasets) and AAC (for the audio dataset). All of the image datasets have integer pixel values between 0 and 255. Accordingly, we round the reconstructions of PBA and PCA to the nearest integer in this range. Figure 4 shows the same tradeoff for PBA and PCA when reconstructions are

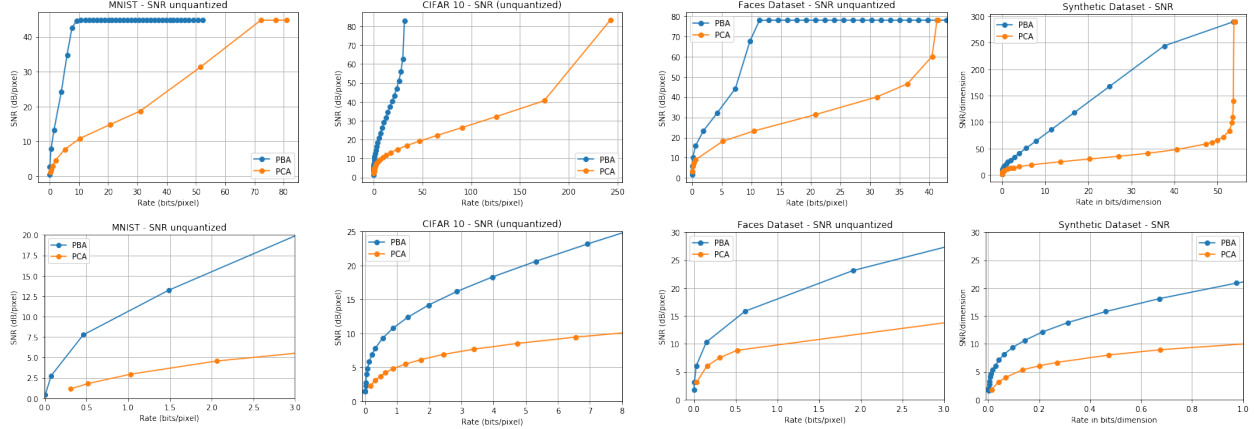


Figure 4: SNR/pixel vs Rate (bits/pixel) for MNIST, CIFAR-10, Faces and Synthetic dataset. Reconstructions are not rounded to integers from 0 to 255. The bottom four plots are zoomed-in versions of the top four plots.

not rounded off to the nearest integer. We see that PBA consistently outperforms PCA and JPEG, and is competitive with JPEG2000, even though the JPEG and JPEG2000 are variable-rate.⁴ We estimate the size of the JPEG header by compressing an empty image and subtract this estimate from all the compression sizes produced by JPEG. We do not plot JPEG2000 performance for MNIST since it requires at least a 32x32 image. For audio data, we observe that PBA consistently outperforms PCA and AAC. Since the image data all use 8 bits per pixel, one can obtain infinite SNR at this rate via the trivial encoding that communicates the raw bits. PCA and PBA do not find this solution because they quantize in the transform domain, where the lattice-nature of the pixel distribution is not apparent. Determining how to leverage lattice structure in the source distribution for purposes of compression is an interesting question that transcends the PBA and PCA algorithms and that we will not pursue here.

The reason that PCA performs poorly is that it favors sending the less significant bits of the most significant components over the most significant bits of less significant components, when the latter are more valuable for reconstructing the source. Arguably, it does not identify the “principal bits.” Figure 5 shows the eigenvalue distribution of the different datasets, and Figure 6 shows the number of distinct components about which information is sent as a function of rate for both PBA and PCA. We see that PBA sends information about many more components for a given rate than does PCA. We discuss the ramifications of this for downstream tasks, such as classification, in Section 5.3.

5.2 SSIM Performance

Structural similarity (SSIM) and Multi-Scale Structural similarity (MS-SSIM) are metrics that are tuned to perceptual similarity. Given two images, the SSIM metric outputs a real value between 0 and 1 where a higher value indicates more similarity between the images. We evaluate the performance of our algorithms on these metrics as well in Figure 7. We see that PBA consistently

⁴It should be noted, however, that JPEG and JPEG2000 aim to minimize subjective distortion, not MSE, and they do not allow for training on sample images, as PBA and PCA do. A similar caveat applies to AAC.

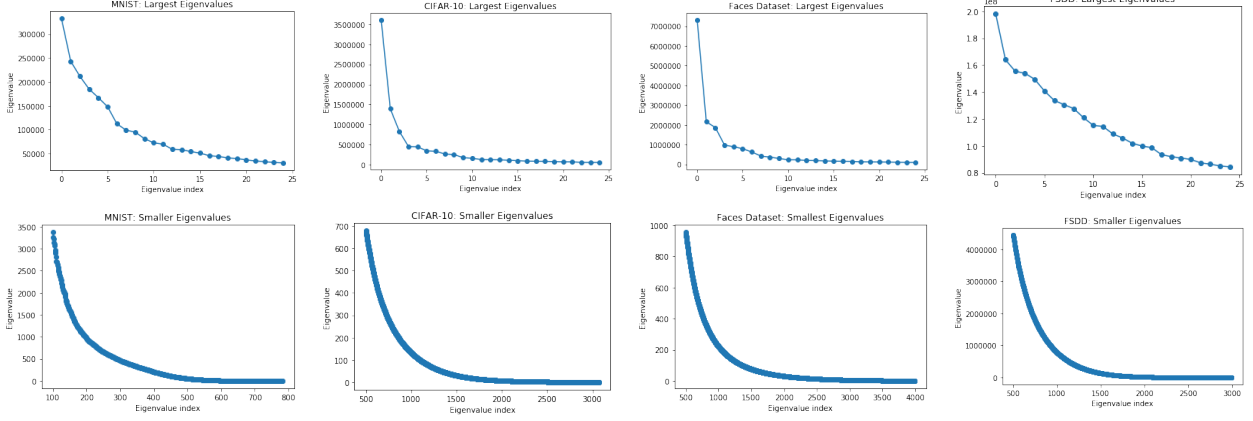


Figure 5: Eigenvalue distribution of the datasets. The top three plots are the largest 25 eigenvalues for MNIST, CIFAR-10, Faces and FSDD dataset. The bottom four figures plot the remaining eigenvalues except the largest 500.

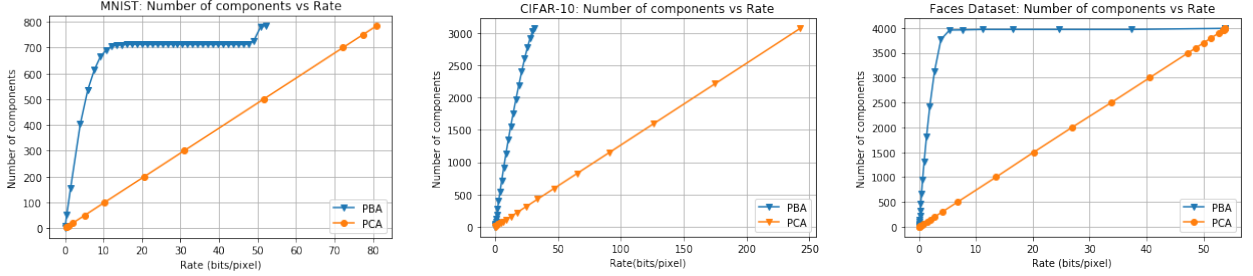


Figure 6: Plots of number of components sent vs rate (bits/pixel) for PBA and PCA.

dominates PCA, and although it was not optimized for this metric, beats JPEG at low rates as well.

5.3 Performance on Downstream tasks

Lastly, we compare the impact of using PBA and PCA on an important downstream task, namely classification. We evaluate the algorithms on MNIST and CIFAR-10 datasets and use neural networks for classification. Our hyperparameter and architecture choices are given in Table 1. We divide the dataset into three parts. From the first part, we obtain the covariance matrix that we use for PCA and to obtain the PBA compressor. The second and third part are used as training and testing data for the purpose of classification. For a fixed rate, reconstructions are passed to the neural networks for training and testing respectively. Since our goal is to compare classification accuracy across the compressors, we fix both the architecture and hyperparameters, and do not perform any additional tuning for the separate algorithms.

Figure 8 shows that PBA outperforms PCA in terms of accuracy. The difference is especially significant for low rates; all algorithms attain roughly the same performance at higher rates.

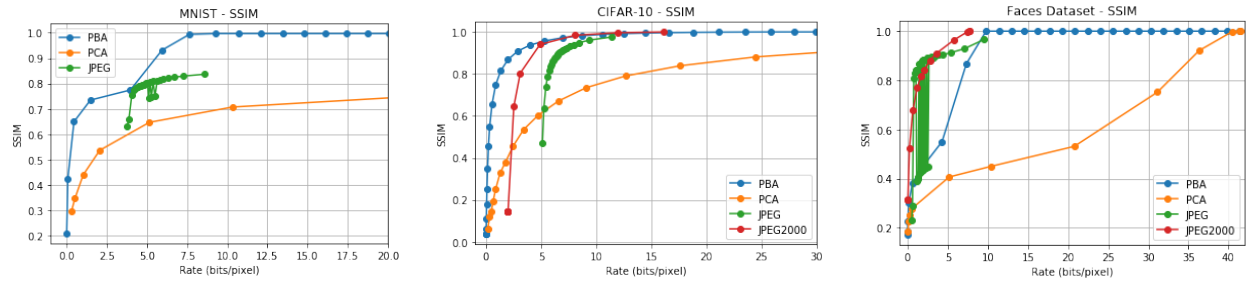


Figure 7: SSIM vs Rate (bits/pixel) for MNIST, CIFAR-10, Faces Dataset

Hyperparameter	MNIST	CIFAR-10
Architecture	2-layer fully connected NN	Convolutional Neural Network with 2 convolutional layers, pooling and three fully connected layers
# Hidden Neurons	100	NA
Optimization Algorithm	Adam	SGD with momentum
Loss	Cross-entropy	Cross-entropy
Learning Rate	0.0005	0.01

Table 1: Hyperparameter Choices and Architecture for Classification

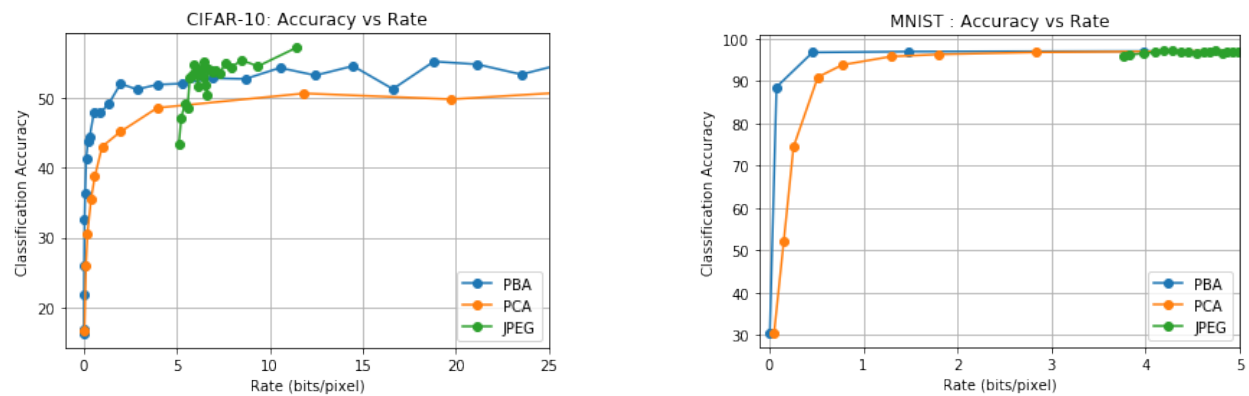


Figure 8: Accuracy vs Rate (bits/pixel) for MNIST, CIFAR-10

References

- [AMT⁺17] Eirikur Agustsson, Fabian Mentzer, Michael Tschannen, Lukas Cavigelli, Radu Timofte, Luca Benini, and Luc V Gool. Soft-to-hard vector quantization for end-to-end learning compressible representations. In *Advances in Neural Information Processing Systems 30*, pages 1141–1151, 2017.
- [AT20] Eirikur Agustsson and Lucas Theis. Universally quantized neural compression. In *Advances in Neural Information Processing Systems 33*, pages 12367–12376, 2020.
- [ATM⁺19] Eirikur Agustsson, Michael Tschannen, Fabian Mentzer, Radu Timofte, and Luc Van Gool. Generative adversarial networks for extreme learned image compression. In *Proceedings of the IEEE International Conference on Computer Vision*, pages 221–231, 2019.
- [BCM⁺20] Johannes Ballé, Philip A Chou, David Minnen, Saurabh Singh, Nick Johnston, Eirikur Agustsson, Sung Jin Hwang, and George Toderici. Nonlinear transform coding. *arXiv:2007.03034*, 2020.
- [Ber99] Dimitri P. Bertsekas. *Nonlinear Programming*. Athena Scientific, 1999.
- [BH89] Pierre Baldi and Kurt Hornik. Neural networks and principal component analysis: Learning from examples without local minima. *Neural Networks*, 2(1):53 – 58, 1989.
- [Bis06] Christopher M. Bishop. *Pattern Recognition and Machine Learning (Information Science and Statistics)*. Springer-Verlag, Berlin, Heidelberg, 2006.
- [BK88] Herve Boursard and Y. Kamp. Auto-association by multilayer perceptrons and singular value decomposition. *Biological Cybernetics*, 59:291–294, 1988.
- [Bla65] Nelson M. Blachman. The convolution inequality for entropy powers. *IEEE Trans. Inf. Theory*, 11(2):267–271, April 1965.
- [BLS16] Johannes Ballé, Valero Laparra, and Eero Simoncelli. End-to-end optimization of nonlinear transform codes for perceptual quality. In *2016 Picture Coding Symposium (PCS)*, 2016.
- [BLSG20] Xuchan Bao, James Lucas, Sushant Sachdeva, and Roger Grosse. Regularized linear autoencoders recover the principal components, eventually. *arXiv:2007.06731*, 2020.
- [BMS⁺18] Johannes Ballé, David Minnen, Saurabh Singh, Sung Jin Hwang, and Nick Johnston. Variational image compression with a scale hyperprior. In *International Conference on Learning Representations*, 2018.
- [BV04] Stephen Boyd and Lieven Vandenberghe. *Convex Optimization*. Cambridge, 2004.
- [CEKL19] Yoojin Choi, Mostafa El-Khamy, and Jungwon Lee. Variable rate deep image compression with a conditional autoencoder. In *Proceedings of the IEEE/CVF International Conference on Computer Vision (ICCV)*, October 2019.
- [CT06] Thomas M. Cover and Joy A. Thomas. *Elements of Information Theory*. Wiley, 2006.

- [HJ13] Roger A. Horn and Charles R. Johnson, editors. *Matrix Analysis*. Cambridge University Press, USA, 2013.
- [HRTC19] Amirhossein Habibian, Ties van Rozendaal, Jakub M Tomczak, and Taco S Cohen. Video compression with rate-distortion autoencoders. In *Proceedings of the IEEE International Conference on Computer Vision*, pages 7033–7042, 2019.
- [HS06] Geoffrey E Hinton and Ruslan R Salakhutdinov. Reducing the dimensionality of data with neural networks. *Science*, 313(5786):504–507, 2006.
- [Jac] Zohar Jackson. Free spoken digit dataset (fsdd). <https://github.com/Jakobovski/free-spoken-digit-dataset>.
- [Kay98] Steven M Kay. *Estimation Theory*. Prentice Hall PTR, 1998.
- [KBGS19] Daniel Kunin, Jonathan Bloom, Aleksandrina Goeva, and Cotton Seed. Loss landscapes of regularized linear autoencoders. In *International Conference on Machine Learning*, volume 97, pages 3560–3569, 2019.
- [Kri09] Alex Krizhevsky. Learning multiple layers of features from tiny images. *Master's Thesis, Department of Computer Science, University of Toronto*, 2009.
- [LBBH98] Yann LeCun, Léon Bottou, Yoshua Bengio, and Patrick Haffner. Gradient-based learning applied to document recognition. *Proceedings of the IEEE*, 86(11):2278–2324, 1998.
- [LNP19] Saïd Ladjal, Alasdair Newson, and Chi-Hieu Pham. A pca-like autoencoder. [abs/1904.01277](https://arxiv.org/abs/1904.01277), 2019.
- [LTGN19] James Lucas, George Tucker, Roger B Grosse, and Mohammad Norouzi. Don't blame the elbow! a linear vae perspective on posterior collapse. In *Advances in Neural Information Processing Systems*, volume 32, pages 9408–9418, 2019.
- [LZW⁺21] Liang Liao, Xuechun Zhang, Xinqiang Wang, Sen Lin, and Xin Liu. Generalized image reconstruction over t-algebra. *arXiv:2101.06650*, 2021.
- [MB95] Alan V. McCree and Thomas P. Barnwell. A mixed excitation lpc vocoder model for low bit rate speech coding. *IEEE Transactions on Speech and Audio Processing*, 3(4):242–250, 1995.
- [MOA11] Albert W. Marshall, Ingram Olkin, and Barry C. Arnold. *Inequalities: Theory of Majorization and its Applications*, volume 143. Springer, 2011.
- [OSWS20] Reza Oftadeh, Jiayi Shen, Zhangyang Wang, and Dylan Shell. Eliminating the invariance on the loss landscape of linear autoencoders. In *International Conference on Machine Learning*, pages 7405–7413, 2020.
- [RB17] Oren Rippel and Lubomir Bourdev. Real-time adaptive image compression. In *International Conference on Machine Learning*, pages 2922–2930, 2017.

- [RZM19] Michal Rolínek, Dominik Zietlow, and Georg Martius. Variational autoencoders pursue pca directions (by accident). In *Proceedings of the IEEE/CVF Conference on Computer Vision and Pattern Recognition (CVPR)*, June 2019.
- [SA85] M. Schroeder and B. Atal. Code-excited linear prediction(celp): High-quality speech at very low bit rates. In *IEEE International Conference on Acoustics, Speech, and Signal Processing*, volume 10, pages 937–940, 1985.
- [San12] Rafael do EspArito Santo. Principal Component Analysis Applied to Digital Image Compression. *Einstein (São Paulo)*, 10:135 – 139, 06 2012.
- [TAL18] Michael Tschannen, Eirikur Agustsson, and Mario Lucic. Deep generative models for distribution-preserving lossy compression. In *Advances in Neural Information Processing Systems 31*, pages 5929–5940. 2018.
- [TOH⁺16] George Toderici, Sean M O’Malley, Sung Jin Hwang, Damien Vincent, David Minnen, Shumeet Baluja, Michele Covell, and Rahul Sukthankar. Variable rate image compression with recurrent neural networks. In *International Conference on Learning Representations*, 2016.
- [TSCH17] Lucas Theis, Wenzhe Shi, Andrew Cunningham, and Ferenc Huszár. Lossy image compression with compressive autoencoders. In *International Conference on Learning Reperesentations*, 2017.
- [TVJ⁺17] George Toderici, Damien Vincent, Nick Johnston, Sung Jin Hwang, David Minnen, Joel Shor, and Michele Covell. Full resolution image compression with recurrent neural networks. In *IEEE Conference on Computer Vision and Pattern Recognition*, pages 5435–5443, 2017.
- [Vor] Vorbis audio compression. <https://xiph.org/vorbis/>. Accessed: 2021-01-26.
- [WBSS04] Zhou Wang, A. C Bovik, H. R. Sheikh, and E. P. Simoncelli. Image quality assessment: From error visibility to structural similarity. *IEEE Transactions on Image Processing*, 13(4):600–612, 2004.
- [ZCG⁺18] Lei Zhou, Chunlei Cai, Yue Gao, Sanbao Su, and Junmin Wu. Variational autoencoder for low bit-rate image compression. In *Proceedings of the IEEE Conference on Computer Vision and Pattern Recognition Workshops*, pages 2617–2620, 2018.
- [ZF92] Ram Zamir and Meir Feder. On universal quantization by randomized uniform/lattice quantizers. *IEEE Trans. Inf. Theory*, 38:428–436, 1992.

A Review of Schur-Convexity

In this section, we review the key definitions and theorems related to Schur-convexity that we use in the proof of Theorem 1.

Definition 7. (Majorization) [HJ13] For a vector $\mathbf{v} \in \mathbb{R}^d$, let \mathbf{v}^\downarrow denote the vector with the same components arranged in descending order. Given vectors $\mathbf{a}, \mathbf{b} \in \mathbb{R}^d$, we say \mathbf{a} majorizes \mathbf{b} and denote $\mathbf{a} \succ \mathbf{b}$, if

$$\sum_{i=1}^d [\mathbf{a}]_i = \sum_{i=1}^d [\mathbf{b}]_i,$$

and for all $k \in [d - 1]$,

$$\sum_{i=1}^k [\mathbf{a}^\downarrow]_i \geq \sum_{i=1}^k [\mathbf{b}^\downarrow]_i.$$

Definition 8. (Schur-convexity) A function $f : \mathbb{R}^d \rightarrow \mathbb{R}$ is Schur-convex if for any vectors $\mathbf{a}, \mathbf{b} \in \mathbb{R}^d$, such that $\mathbf{a} \succ \mathbf{b}$,

$$f(\mathbf{a}) \geq f(\mathbf{b}).$$

f is strictly Schur-convex if the above inequality is a strict inequality for any $\mathbf{a} \succ \mathbf{b}$ that are not permutations of each other. f is Schur-concave if the direction of the inequality is reversed and is strictly Schur concave if the direction of the inequality is reversed and it is a strict inequality for any $\mathbf{a} \succ \mathbf{b}$ that are not permutations of each other.

Proposition 9. [MOA11] If $f : \mathbb{R} \rightarrow \mathbb{R}$ is convex, then $\phi : \mathbb{R}^d \rightarrow \mathbb{R}$ given by

$$\phi(\mathbf{v}) = \sum_{i=1}^d f([v]_i)$$

is Schur-convex. If f is concave, then ϕ is Schur-concave. Likewise if f is strictly convex, ϕ is strictly Schur-convex and if f is strictly concave, ϕ is strictly Schur-concave.